Hepatic recruitment of CD11b$^+$Ly6C$^+$ inflammatory monocytes promotes hepatic ischemia/reperfusion injury

PENG SONG[1], JUNBIN ZHANG[2], YUNWEI ZHANG[2], ZHIPING SHU[3], PENG XU[2], LONG HE[4], CHAO YANG[1], JINXIANG ZHANG[2], HUI WANG[5], YIQING LI[1] and QIN LI[1]

Departments of [1]Vascular Surgery and [2]Emergency Surgery, Union Hospital; [3]Department of Nuclear Medicine, Tongji Hospital; [4]Department of Clinical Laboratory, Puai Hospital, Tongji Medical College; [5]Department of Genetics, Tongji Medical College, Huazhong University of Science and Technology, Wuhan, Hubei 430033 P.R. China

Received November 23, 2016; Accepted November 24, 2017

DOI: 10.3892/ijmm.2017.3315

Abstract. Monocytes infiltrate damaged liver tissue during noninfectious liver injury and often have dual roles, perpetuating inflammation and promoting resolution of inflammation and fibrosis. However, how monocyte subsets distribute and are differentially recruited in the liver remain unclear. In the current study, the subpopulations of infiltrating monocytes were examined following liver ischemia/reperfusion (I/R) injury in mice using flow cytometry. CD11b$^+$Ly6C high (Ly6C^{hi}) cells (inflammatory monocytes) and CD11b$^+$Ly6C low cells (reparative monocytes) were recruited into the liver following I/R injury. Treatment with clodronate-loaded liposomes, which transiently deplete systemic macrophages, alleviated hepatic damage. Mice genetically deficient in C-C motif chemokine ligand 2 (CCL2), or its receptor C-C chemokine receptor 2 (CCR2), exhibited diminished hepatic damage compared with wild-type mice following I/R, by controlling intrahepatic inflammatory Ly6C^{hi} monocyte accumulation. In addition, the CCR2 specific inhibitor RS504393 alleviated hepatic I/R injury. The results suggest that the CCR2/CCL2 axis has an important role in monocyte infiltration and may represent a novel target for the treatment of liver I/R injury.

Introduction

Liver ischemia/reperfusion (I/R) injury is an important cause of liver damage occurring during liver surgery or transplantation, and significantly influences the prognosis of liver function (1). A variety of immune cells, including monocytes, Kupffer cells, CD4$^+$ lymphocytes, neutrophils, hepatocytes, and cytokines are involved in liver I/R injury (2-4). Hepatic macrophages have an important role in maintaining homeostasis of the liver and in the pathogenesis of liver injury. I/R can cause the activation of Kupffer cells to release transforming growth factor-α, and other pro-inflammatory cytokines, including tumor necrosis factor-α (TNF-α) and interleukin-6 (IL-6). An increase in the inflammatory state results in the activation of the immune system as a major intermediary during the process of I/R injury (5), which can drive injury resolution or lead to chronic inflammation (6,7).

Intrahepatic monocyte infiltration of the damaged liver tissue represents an important constitution of the innate immune response (8). When the liver is under pathological stress, such as steatohepatitis and viral hepatitis, Kupffer cells can differentiate from infiltrated bone marrow-derived mononuclear cells (9). In addition, it has been reported that Kupffer cells can be constantly replenished by blood monocytes, even in steady state conditions (10). Two major monocyte subsets in mice have been identified that closely resemble human monocytes and vary in migratory and differentiation properties (11). In humans, classical CD14$^+$CD16$^+$ monocytes express C-C chemokine receptor 2 (CCR2), CD64, and selectin L, whereas non-classical CD14$^+$CD16$^-$ monocytes lack CCR2 (12). Their counterparts in mice are CCR2$^+$Ly6C high (Ly6C^{hi}) and CCR2$^-$Ly6C low (Ly6C^{lo}) monocytes, respectively (12,13). Ly6C^{hi} monocytes are considered to be precursors to macrophages and dendritic cells during inflammatory conditions, whereas Ly6C^{lo} monocytes represent steady state precursor cells for tissue macrophages (14-16). The differential recruitment of these monocyte subsets appears to be crucially controlled by chemokines released from injured tissue (17-19). As such, enhanced hepatic expression of the ligands for CCR2, including monocyte chemoattractant protein-1 (MCP-1)/C-C motif chemokine ligand 2 (CCL2), CCR6 and macrophage inflammatory protein-3α/CCL20, has been reported in patients with liver cirrhosis (17,20).

CCR2 is the specific receptor for MCP-1/CCL2, but is also the receptor for CCL7, CCL8, CCL11, CCL12 and CCL13. Recently, CCL2 has been reported to have a critical role in the pathogenesis of various liver diseases (21-23). CCL2 interacts with its

Correspondence to: Dr Yiqing Li or Dr Qin Li, Department of Vascular Surgery, Union Hospital, Huazhong University of Science and Technology, 1277 Jiefang Avenue, Wuhan, Hubei 430030, P.R. China
E-mail: qzg599@126.com
E-mail: 16091515@qq.com

Abbreviations: I/R injury, ischemia/reperfusion injury; CCR2, C-C chemokine receptor 2; CCL2, C-C motif chemokine ligand 2; Ly6C^{hi}, Ly6C high; Ly6C^{lo}, Ly6C low; ALT, alanine aminotransferase; AST, aspartate aminotransferase; NPCs, non-parenchymal cells; WT, wild-type; TNF-α, tumor necrosis factor-α; IL-6, interleukin-6

Key words: C-C motif chemokine ligand 2, C-C chemokine receptor 2, ischemia/reperfusion, inflammatory monocyte

receptor, CCR2, and induces mononuclear cells in the blood to cross the endothelial barrier towards sites of inflammation during an inflammatory response (24). Upregulated expression of CCL2 has been reported in various liver diseases (21,25). Although the CCR2/CCL2 interaction has been reported to be associated with various liver diseases (26), the underlying mechanism of this association has not been clearly elucidated. Specifically, the role of CCL2/CCR2 in the immune response of the liver during I/R injury remains unknown. The current study aimed to identify the infiltrating monocyte subsets in liver I/R injury and determine how the CCL2/CCR2 axis contributes to the hepatic monocyte recruitment during I/R injury.

Materials and methods

Animals. Male C57BL/6 mice [wild-type (WT); weight, 22-25 g] were purchased from the Center for Animal Experiment of Wuhan University (Wuhan, China). Male CCL2$^{-/-}$ or CCR2$^{-/-}$ C57BL/6 mice were bred at the sterile Animal Management Centre of Tongji Medical College (Wuhan, China) and used between the ages of 8-12 weeks. The original experiments used 10 mice/group [including hematoxylin and eosin (H&E) staining, serum levels of alanine aminotransferase (ALT) and aspartate aminotransferase (AST), mRNA/protein levels of TNF-α and IL-6 in liver tissue; recruitment of monocytes into I/R injured liver lobes; effect of macrophage depletion as well as CCR2 or CCL2 knockout on liver I/R injury]. For the additional experiments performed (quantification of intrahepatic CD4$^+$ T cells and CD8$^+$ T cells; immunofluorescence staining of hepatic infiltrated monocyte subsets; effect of CCR2 inhibition on hepatic I/R injury), 4-6 animals were used per group. All animal studies were performed in accordance with the National Institutes of Health Guidelines for Care and Use of Laboratory Animals and were approved by the Scientific Affairs Committee on Animal Research and Ethics of Tongji Hospital, Tongji Medical College, Huazhong University of Science and Technology (Wuhan, China).

Liver I/R model. A non-lethal model of segmental (70%) hepatic warm ischemia was performed as described previously (27). Briefly, mice were anesthetized with sodium pentobarbital [60 mg/kg; intraperitoneally (i.p.)], which is a traditional anesthetic used in animal research of liver, lung or cardiac I/R injury (28-30). A midline laparotomy was performed and ligaments surrounding each lobe were dissected carefully. The portal vein, the hepatic artery, and the bile duct supplying the median and the left lateral lobes of the liver were clamped with an artery clip. The caudal and right lobes retained portal and arterial inflow and venous outflow, preventing intestinal venous congestion. Following surgery, the abdominal cavity was properly closed and then the mice were placed in an incubator maintained at 32˚C. Liver lobes were inspected for ischemia by visualizing the pale blanching of the ischemic lobes intermittently. After 60 min, the clamps were removed and liver reperfusion was initiated. For sham controls, the animals underwent anesthesia, laparotomy, and exposure of the portal triad without hepatic I/R. Mice were sacrificed after 6 h of reperfusion. Blood and tissues of liver lobes from sham and I/R injury mice were collected and stored at -80˚C for future analysis.

Serum transaminase. Cardiac puncture blood was collected following hepatic I/R or sham into tubes (without anticoagulant), allowed to clot and serum was separated by centrifugation at 200 x g at 4˚C for 10 min. For CCR2 inhibitor pretreatment, mice were injected with RS-504393 (25 mg/kg; Sigma-Aldrich; Merck KGaA, Darmstadt, Germany) or dimethyl sulfoxide (DMSO) 1 h prior to I/R injury. Liver injury was estimated by measuring the increased activities of serum ALT and AST, which were measured using a Synchron CX7 analyzer (Beckman Coulter, Inc., Brea, CA, USA) in the Clinical Biochemical Laboratory of Wuhan Union Hospital (Wuhan, China).

Histopathology. At predetermined time points (6 h after reperfusion), mice were sacrificed humanely by CO_2 suffocation. The liver lobes were collected from I/R mice and sham mice and fixed in 4% formalin at room temperature (25˚C) for 4 h. Fixed tissues were embedded in paraffin, cut into 5 μm thick sections and were placed onto glass slides. Slides were then stained with hematoxylin and eosin (H&E) using a conventional protocol. The necrotic area was assessed by 2 independent pathologists, and more than 10 random fields of view were quantified using the Image-Pro Plus v 6.0 software (Media Cybernetics, Silver Spring, MD, USA).

Reverse transcription-quantitative polymerase chain reaction (RT-qPCR). Total RNA was extracted from the lobes of the ischemic and sham liver using TRIzol. RT was performed using the RT kit (Thermo Fisher Scientific, Inc., Waltham, MA, USA) at 65˚C for 5 min. qPCR was performed using the SYBR-Green PCR mix (Thermo Fisher Scientific, Inc.) in a LightCycler 480 system (Roche Molecular Diagnostics, Pleasanton, CA, USA). The PCR program was 95˚C, 2 min, x1; 95˚C, 10 sec, 60˚C, 1 min, x40. β-actin was used as an internal reference. Many previous I/R studies (31,32) also used this gene for data normalization, indicating I/R has no effect on the expression of β-actin. Primers were synthesized by Sangon Biotech Co., Ltd. (Shanghai, China) and the sequences were as follows: TNF-α, 5'-ACTGAACTTCGGGGT GATCG-3' (forward) and 5'-GGCTACAGGCTTGTC ACTCG-3' (reverse); IL-6, 5'-AGTTGCCTTCTTGGG ACTGA-3' (forward) and 5'-TCCACGATTTCCCAG AGAAC-3' (reverse); β-actin, 5'-GTGACGTTGACATCCGTA AAGA-3' (forward) and 5'-GCCGGACTCATCGTACTCC-3' (reverse). Data were analyzed using the $2^{-\Delta\Delta Cq}$ method (33).

Serum/liver cytokines. The serum expression levels of TNF-α and IL-6 was measured using commercial ELISA kits [TNF-α (MTA00B); IL-6 (M6000B); R&D Systems, Inc., Minneapolis, MN, USA] following standardized techniques (34). All samples and standards were performed in duplicate. ELISA was also performed on tissues of liver lobes from sham and I/R mice.

Isolation of hepatic non-parenchymal cells (NPCs). Hepatic NPCs were obtained from the liver using a collagenase digestion method, as described previously (35). Briefly, the animals were anesthetized and the liver was perfused *in situ* by way of the portal vein with PBS containing 0.05% collagenase. The liver was removed, placed in PBS and incubated at 37˚C for 15 min. The incubated liver was then torn using cell scrapers. The cell suspension were shaken on a shaking table at 37˚C

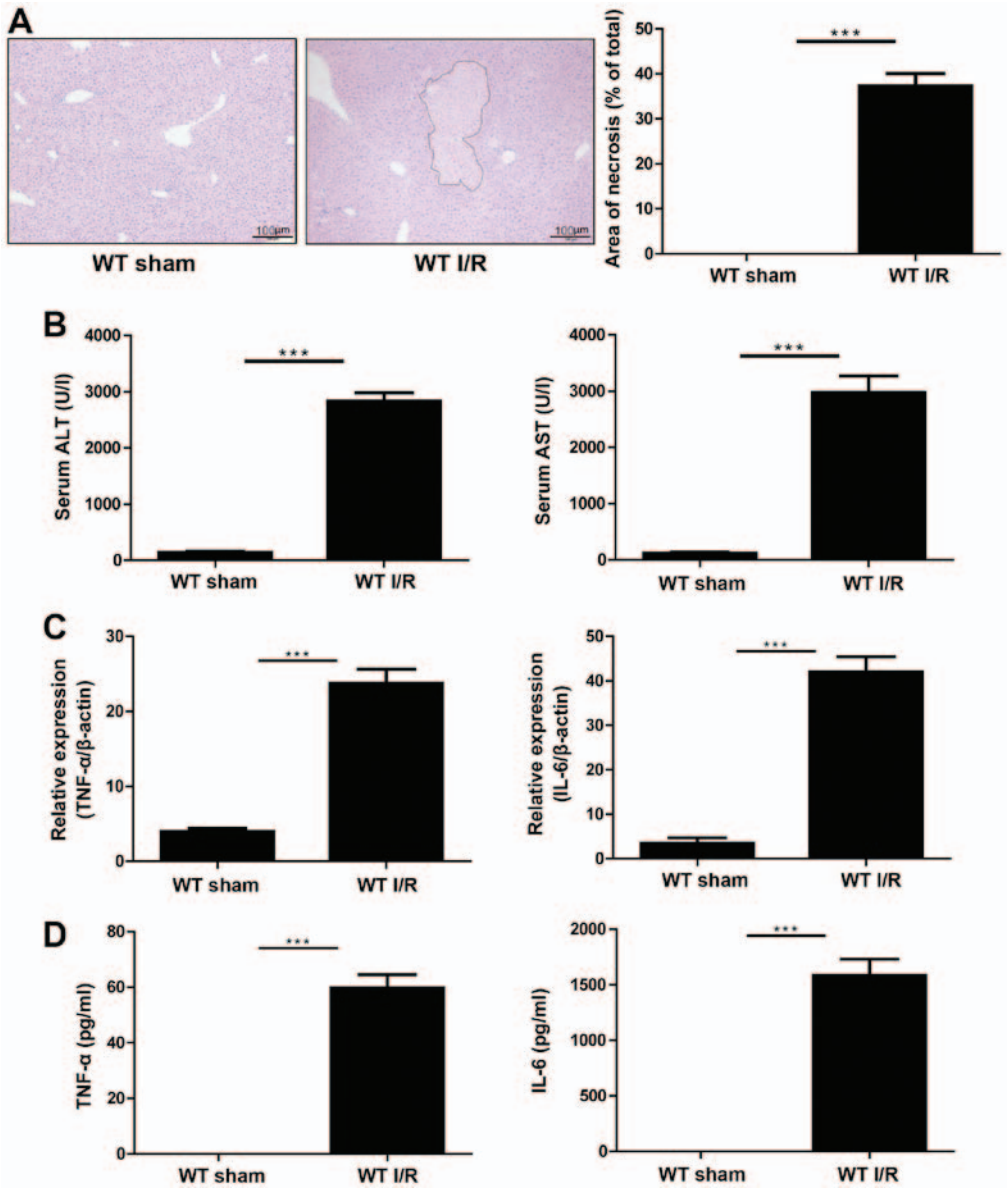

Figure 1. Non-lethal model of segmental (70%) warm liver I/R injury in mice. (A) Liver hematoxylin and eosin staining of mice in the WT sham and I/R injury group. Images are representative of 10 animals per group. (B) Serum levels of ALT and AST in WT sham or I/R injury mice. (C) mRNA levels of TNF-α and IL-6 in WT sham or I/R injury liver tissue. (D) Protein levels of TNF-α and IL-6 in WT sham or I/R injury liver tissue. Data are presented as the mean + standard error. ***P<0.001. WT, wild-type; I/R, ischemia/reperfusion; ALT, alanine aminotransferase; AST, aspartate aminotransferase; TNF-α, tumor necrosis factor-α; IL-6, interleukin-6.

for 20 min and then filtered through a 70-μm nylon mesh. NPCs were isolated by gradient centrifugation at 400 x g for 16 min with acceleration and braking at 0 using OptiPrep™ (Axis-Shield Diagnostics Ltd., Dundee, UK) according to manufacturer's instructions. NPCs were then washed by high-speed centrifugation (1,500 rpm for 5 min).

Depletion of Kupffer cells. Kupffer cells were depleted by using clodronate in a liposomal formulation (36,37). Briefly, a dose of 0.2 ml/20 g animal body weight of liposome-encapsulated clodronate (FormuMax Scientific, Inc., Sunnyvale, CA, USA) was i.p. injected 48 h before I/R. Macrophage depletion was successfully achieved (~90%), as examined by flow cytometry (anti-F4/80-PerCP-Cy5.5, clone BM8 (cat. no. 123128); from BioLegend, Inc., San Diego, CA, USA) in the liver 48 h after a single injection.

Flow cytometric analysis. Red blood cells in the isolated NPCs were lysed using Hybri-Max red blood cell lysis buffer (Sigma-Aldrich; Merck KGaA). Cell numbers were determined by a sequential gating scheme. The cells were then incubated with fluorescent-labeled anti-mouse antibodies in PBS containing 1% bovine serum albumin for 30 min at 4˚C. Antibodies used in this experiment were as follows: anti-CD45-Pacific Blue (clone 30-F11; cat. no. 103126), anti-Ly6C-APC-Cy7 (clone HK1.4; cat. no. 128026), anti-CD11b-PE-Cy7 (clone M1/70; cat. no. 101216), and anti-CD4-PerCP-Cy5.5 (clone GK1.5; cat. no. 100434) from BioLegend; anti-CD8-APC (clone 53-6.7; cat. no. 561093) from BD Biosciences (San Diego, CA, USA); anti-CD3-PE-Cy7 (clone 17A2; cat. no. 100220) from BioLegend, Inc. For intracellular cytokine staining, NPCs were isolated following sham or I/R injury of the 3 groups of mice (n=4-6 mice/group) and cultured with GolgiStop (cat. no. 554724;

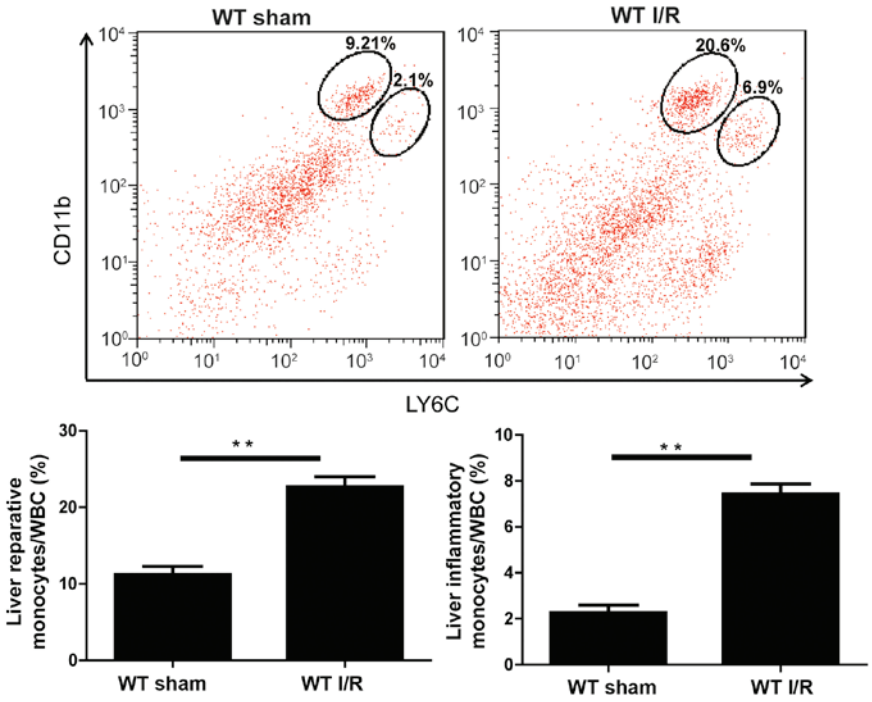

Figure 2. Recruitment of monocytes into I/R injured liver lobes. Isolated hepatic non-parenchymal cells were stained for CD11b and Ly6C and analyzed by flow cytometry. CD11b^{+} Ly6C low (Ly6C$^{lo;}$ bottom left) population represents reparative monocytes and CD11b^{+} Ly6C high (Ly6C^{hi}; bottom right) subset represents inflammatory monocytes. Flow cytometric plots are representative of 10 animals of each group and data are presented as the mean + standard error. **P<0.01. WT, wild-type; I/R, ischemia/reperfusion.

BD Biosciences) for 6 h. The cells were then stained with CD11b, Ly6C and anti-TNF-α-PE (IC410P) from R&D Systems. The corresponding isotype IgGs were used when necessary as controls. Following staining, cells were washed, fixed in 1% paraformaldehyde in 1X PBS, and resuspended at ~5x10^{6}/ml for flow cytometry. Cells were analyzed on a CyAn ADP analyzer (Beckman Coulter, Inc.). FlowJo version 7.6 software (Tree Star, Inc., Ashland, OR, USA) was used to analyze the data (38).

Data analysis. The results were expressed as the mean ± standard error. Student's t-test was used to compare the difference between two groups. For multigroup comparison, one-way analysis of variance was used followed by post hoc Mann Whitney U-test. All of the data analysis was performed using SPSS 15.0 software (SPSS, Inc., Chicago, IL, USA). P<0.05 was considered to indicate a statistically significant difference.

Results

Hepatic pathology in I/R injured liver. Compared with sham animals with normal liver histology, mice undergoing I/R injury exhibited periportal necrosis after 6 h, as determined by H&E staining (Fig. 1A). I/R-induced liver injury was also indicated by elevated serum levels of ALT and AST (Fig. 1B). The levels of inflammatory cytokines TNF-α and IL-6 were significantly higher in liver tissues of I/R mice than in sham animals at the mRNA (Fig. 1C) and protein (Fig. 1D) levels. For the positive control, mice were treated with CCl4 (0.3 ml/kg) and elevated TNF-α and IL-6 in liver tissue were observed (data not shown).

Ly6 high (Ly6C^{hi}) and low (Ly6C^{lo})monocytes are increased in I/R-injured livers. To investigate the cells that secrete the cytokines demonstrated, the population of intrahepatic leukocytes present in the damaged liver was characterized. The flow cytometric plots of CD11b and Ly6C expression in isolated hepatic NPCs from one sham mouse and one I/R mouse, representative of the 10 mice in each group, are presented in Fig. 2. The population of CD11b^{+}Ly6C^{hi} cells (inflammatory monocytes) increased following I/R injury, from 2.1 to 6.9% of CD45^{+} immune cells. CD11b^{+}Ly6C^{lo} cells (reparative monocytes) also increased from 9.21 to 20.6% of CD45^{+} immune cells following hepatic I/R injury (Fig. 2). Statistical analysis was then calculated based on data from all animals of each group and there was significant difference in CD11b^{+}Ly6C$^{hi/low}$ populations between the sham group and I/R group. These results suggest that the increased infiltration of monocytes into liver may have an important role in hepatic pathology in I/R-injured liver.

Treatment with clodronate-loaded liposomes alleviates liver I/R injury. To determine whether monocyte-derived subsets actively promote liver damage or represent an elemental reaction following I/R injury, WT mice were treated with clodronate-loaded liposomes to transiently deplete systemic macrophages 48 h before I/R injury (39). As presented in Fig. 3A, the population of CD11b^{+}Ly6C^{hi} cells in I/R model mice decreased from 7.1 to 0.18% following pretreatment with clodronate-loaded liposomes. CD11b^{+}Ly6C^{lo} cells also decreased from 20.4 to 2.9% in macrophage-depleted mice (Fig. 3A). Following macrophage depletion by clodronate-loaded liposomes, I/R-induced hepatic necrosis was also dramatically decreased (Fig. 3B). Serum ALT and AST levels were also reduced in mice pretreated with clodronate-loaded liposome compared to animals pretreated with PBS (Fig. 3C). These results suggest that the recruitment

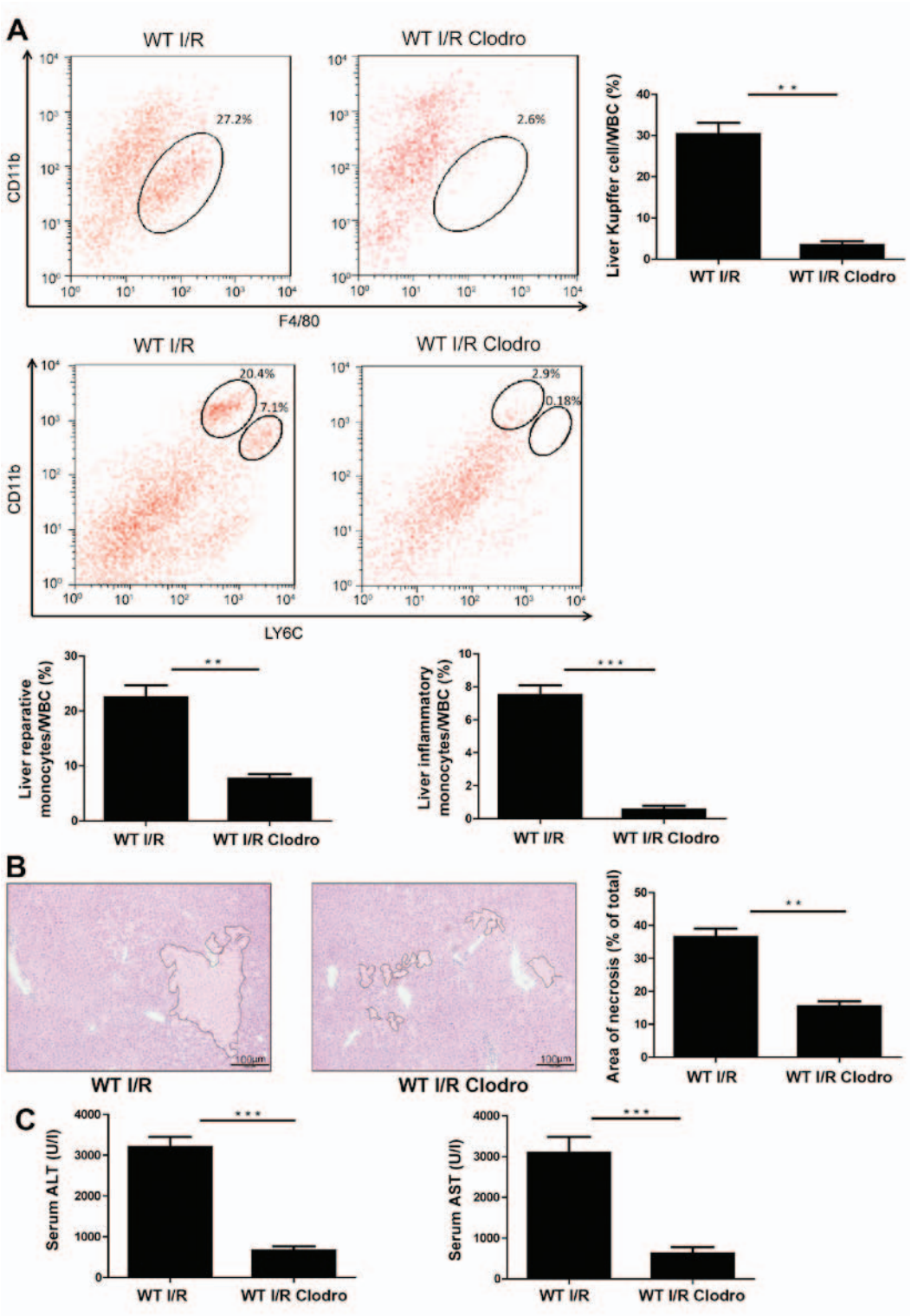

Figure 3. Macrophage depletion alleviates liver I/R injury. Mice were pretreated with clodronate (200 μl/20 g, intraperitoneal) or the same volume of PBS and then subjected to liver I/R injury (n=10 per group). (A) Flow cytometry analysis of the reparative monocytes [CD11b$^+$ Ly6C low (Ly6C^{lo}), reparative monocytes] and inflammatory monocytes [CD11b$^+$ Ly6C high (Ly6C^{hi}), inflammatory monocytes] in liver lobes. (B) Hematoxylin and eosin staining of the liver tissues in I/R injured animals with or without clodronate pretreatment. Areas of necrosis were measured by PhotoImpact 5.0 software (Ulead Systems). (C) Serum levels of ALT and AST in I/R injury mice. Data are presented as the mean ± standard error of each group. **P<0.01 and ***P<0.001. WT, wild-type; I/R, ischemia/reperfusion; Clodro, clodronate; WBC, white blood cells; ALT, alanine aminotransferase; AST, aspartate aminotransferase.

of monocyte subsets into the injured liver may contribute to acute hepatic damage.

CCR2/CCL2 axis is critical for the recruitment of Ly6C$^+$ intrahepatic monocyte-derived cells. Ly6C$^+$ monocytes express high levels of CCR2, CCR1 and CCR6 (39,40). To elucidate the role of CCR2-CCL2 axis in the recruitment of monocytes to damaged liver tissue, I/R-induced liver injury and intrahepatic recruitment of Ly6C$^+$ monocytes were examined in WT, CCR2$^{-/-}$ and CCL2$^{-/-}$ mice. Compared with WT

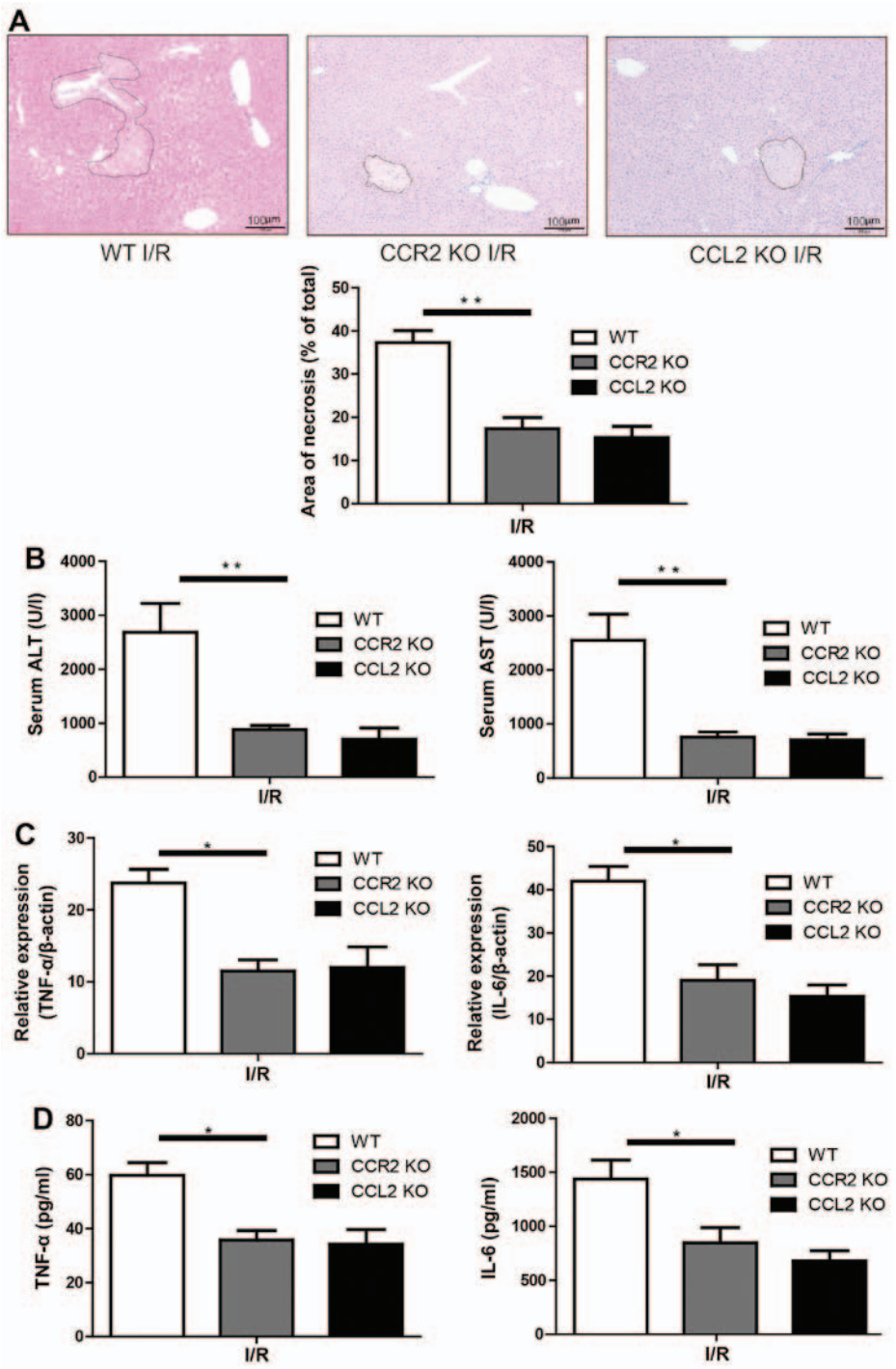

Figure 4. Knockout of CCR2 or CCL2 alleviates liver I/R injury. (A) Three groups of C57BL/6 mice WT, CCR2$^{-/-}$ and CCL2$^{-/-}$(n=10/group] were subjected to non-lethal segmental warm hepatic I/R injury. The liver lobes were hematoxylin and eosin stained and areas of necrosis were quantified. (B) Serum levels of ALT and AST in CCR2$^{-/-}$, CCL2$^{-/-}$ or WT I/R injured mice. (C) mRNA levels of TNF-α and IL-6 in CCR2$^{-/-}$, CCL2$^{-/-}$ or WT I/R injured mice. (D) Protein levels of TNF-α and IL-6 in the liver tissues of CCR2$^{-/-}$, CCL2$^{-/-}$ or WT I/R injured mice. The results are presented as the mean + standard error of each group. *P<0.05 and **P<0.01. WT, wild-type; I/R, ischemia/reperfusion; CCR2, C-C chemokine receptor 2; KO, knockout; CCL2, C-C motif chemokine ligand 2; ALT, alanine aminotransferase; AST, aspartate aminotransferase; TNF-α, tumor necrosis factor-α; IL-6, interleukin-6.

mice that exhibited significant hepatic necrosis, CCR2$^{-/-}$ and CCL2$^{-/-}$ mice exhibited lower levels of necrosis following I/R injury (Fig. 4A). Serum ALT and AST levels were also decreased compared with the WT group (Fig. 4B). The levels of inflammatory cytokines, TNF-α and IL-6, were also decreased in the CCR2$^{-/-}$ and CCL2$^{-/-}$ mice (Fig. 4C and D). In addition, leukocyte infiltration was significantly reduced following injury in CCR2 or CCL2 deficient mice (Fig. 5A). There was a significantly lower accumulation of intrahepatic CD11b^{+}Ly6C^{+} monocytes in CCR2$^{-/-}$ and CCL2$^{-/-}$ mice undergoing I/R. The percentage of CD11b^{+}Ly6C^{hi} inflammatory monocytes and CD11b^{+}Ly6C^{lo} reparative monocytes were decreased in CCR2$^{-/-}$ and CCL2$^{-/-}$ mice compared with WT mice (Fig. 5A). However, there was no difference in the number of CD11b^{+}Ly6C^{hi} cells between CCR2$^{-/-}$ and CCL2$^{-/-}$ sham group and the operation group (Fig. 5). Flow cytometric

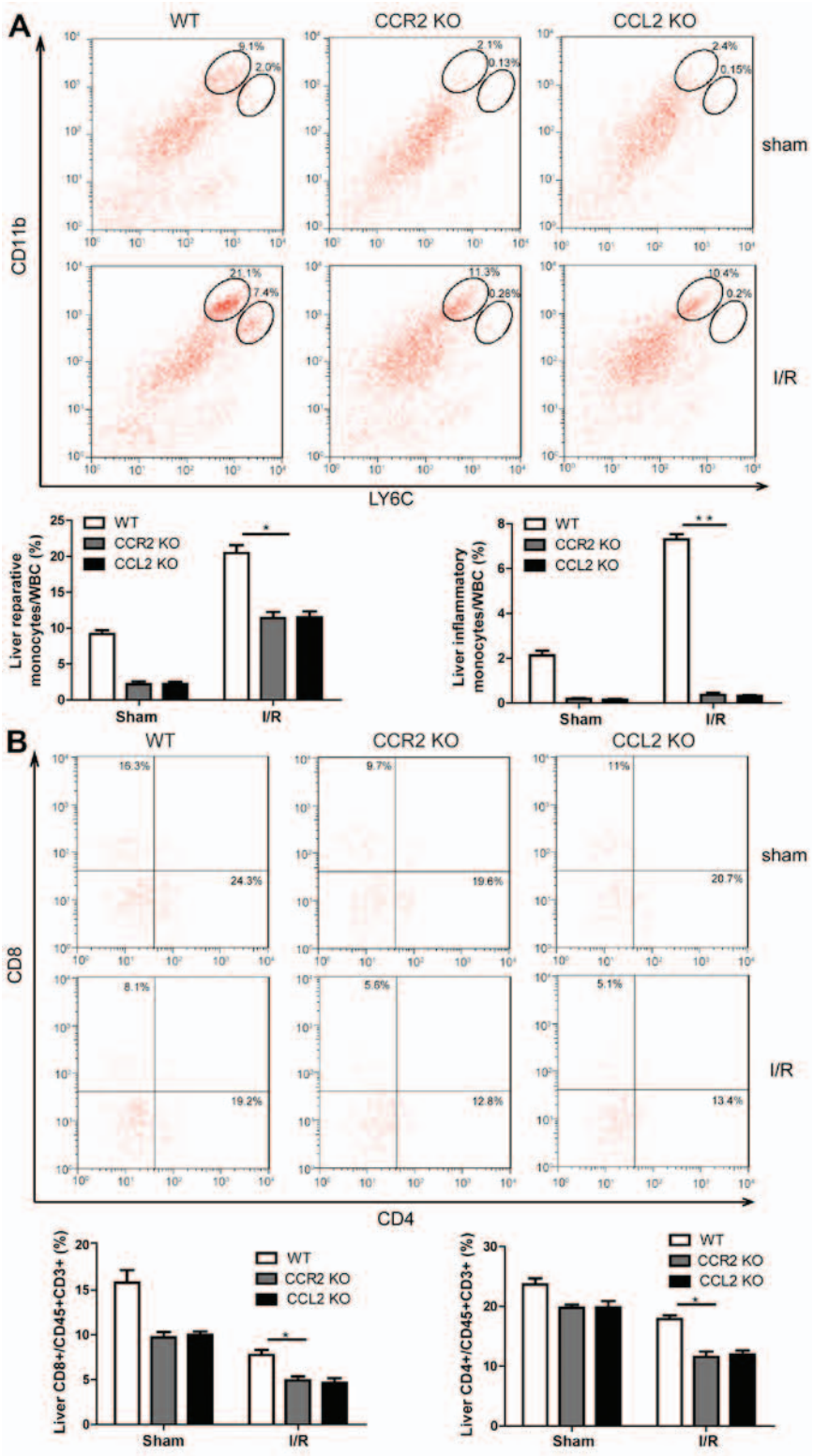

Figure 5. Intrahepatic recruitment of CD11b+Ly6C$^+$ monocytes and decrease of CD4$^+$ and CD8$^+$ T cells in CCR2 or CCL2 knockout mice underwent I/R injury. (A) Hepatic NPCs were isolated from CCR2$^{-/-}$, CCL2$^{-/-}$ or WT mice and then stained with CD11b and Ly6C for flow cytometric analysis. The plots are representative of 10 animals of each group and data are presented as the mean + standard error. *P<0.05 and **P<0.01. (B) Flow cytometric quantification of CD4$^+$ T cells and CD8$^+$ T cells in mice of different genotypes underwent hepatic I/R injury (n=4-6 mice/group). NPCs were first gated by CD45$^+$CD3$^+$, then by CD4$^+$ and CD8$^+$, respectively. The results are presented as the mean + standard error of each group. *P<0.05. WT, wild-type; I/R, ischemia/reperfusion; CCR2, C-C chemokine receptor 2; KO, knockout; CCL2, C-C motif chemokine ligand 2; NPCs, non-parenchymal cells.

quantification also demonstrated that CCR2 or CCL2 knockout decreased the accumulation of CD4$^+$ T cells and CD8$^+$ T cells in mice that underwent hepatic I/R injury (Fig. 5B). The decrease in CD11b$^+$Ly6C$^+$ cells was also revealed by immunofluorescence staining of infiltrated monocyte subsets in injured liver tissue (Fig. 6A). Intracellular cytokine staining demonstrated that CCR2$^{-/-}$ or CCL2$^{-/-}$ mice had significantly lower levels of TNF-α than WT mice following I/R injury,

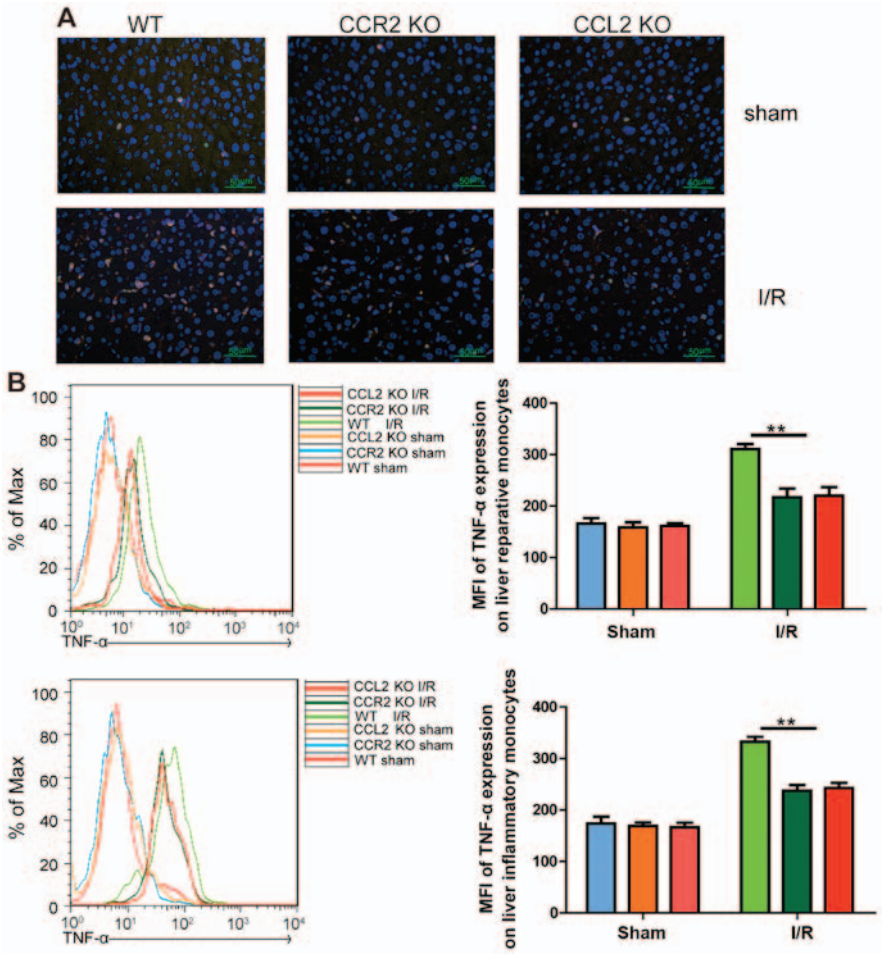

Figure 6. Immunofluorescence staining of infiltrated monocyte subsets in injured liver tissue and quantification of TNF-α in mice of different genotypes by flow cytometry. (A) Double immunofluoroscence staining of CD11b (red) and Ly6C (green) in the sham-operated and I/R-induced liver tissues of WT, CCR2 KO, and CCL2 KO mice (n=4-6 mice/group). The section was then nuclear counter stained with DAPI. Scale bar, 50 μm. (B) Non-parenchymal cells were isolated following sham or I/R injury of the three groups of mice (n=4-6 mice/group) and cultured with GolgiStop for 6 h. The cells were then stained with CD11b, Ly6C and TNF-α. The MFI of TNF-α was measured in both reparative monocytes (CD11b$^+$ Ly6C low; upper panels) and inflammatory monocytes (CD11b$^+$ Ly6C high; lower panels) by flow cytometry. Statistical analysis of TNF-α MFI is presented as the mean + standard error of each group. **P<0.01. WT, wild-type; I/R, ischemia/reperfusion; CCR2, C-C chemokine receptor 2; KO, knockout; CCL2, C-C motif chemokine ligand 2; TNF-α, tumor necrosis factor-α; MFI, mean fluorescence intensity.

whereas there was no induction of TNF-α in the three groups under sham conditions (Fig. 6B).

CCR2 inhibitor alleviates hepatic I/R injury. CCR2$^{-/-}$ or CCL2$^{-/-}$ mice exhibited decreased hepatic I/R injury compared with WT mice. CCR2 has a crucial role in the CCR2/CCL2 axis and certain CCR2 inhibitors have been reported to provide renal and glycemic benefits (41). It was tested whether a CCR2 inhibitor could alleviate hepatic I/R injury. When mice were pretreated with the specific CCR2 inhibitor, RS504393 (25 mg/kg), serum ALT and AST levels were significantly decreased, compared with the control group and vehicle group (Fig. 7A). The CCR2 inhibitor group also exhibited a decrease in the area of necrosis (Fig. 7B). In addition, inflammatory CD11b$^+$Ly6C^{hi} and reparative CD11b$^+$Ly6C^{lo} cells were markedly decreased following RS504393 treatment (Fig. 7C). Similar to the magnitude of inhibition in CCR2$^{-/-}$ deficient mice, CCR2 inhibition nearly entirely suppressed CD11b$^+$Ly6C^{hi} cells infiltration into the hepatic tissue after I/R injury. No difference in CD11b$^+$Ly6C^{hi} and CD11b$^+$Ly6C^{lo} cell populations was observed between the untreated control group and DMSO control group. These results demonstrate that CCR2 inhibition efficiently alleviated hepatic I/R injury and, thus, may be an effective potential drug for hepatic I/R injury.

Discussion

In the present study, the role of infiltrating monocyte subsets into the liver following liver I/R injury was investigated and demonstrated an important functional role for inflammatory CD11b$^+$Ly6C$^+$ monocytes in causing liver I/R injury. The CCR2/CCL2 axis has a critical role in mediating monocyte infiltration into the liver following I/R injury.

Immune cells, and the release of associated cytokines, have been reported to be involved in the occurrence of liver I/R injury, however the exact immunocyte populations have yet to be determined (42). Inflammatory cells also have a major role in liver repair and are recruited immediately following injury (43). CD11b$^+$Ly6C$^+$ and CD11b$^+$Ly6C$^-$ monocytes are the two most well-defined subsets of monocytes and have been proposed to infiltrate tissues during inflammation (44,45). The infiltration of CD11b$^+$Ly6C$^+$ monocyte subset has been

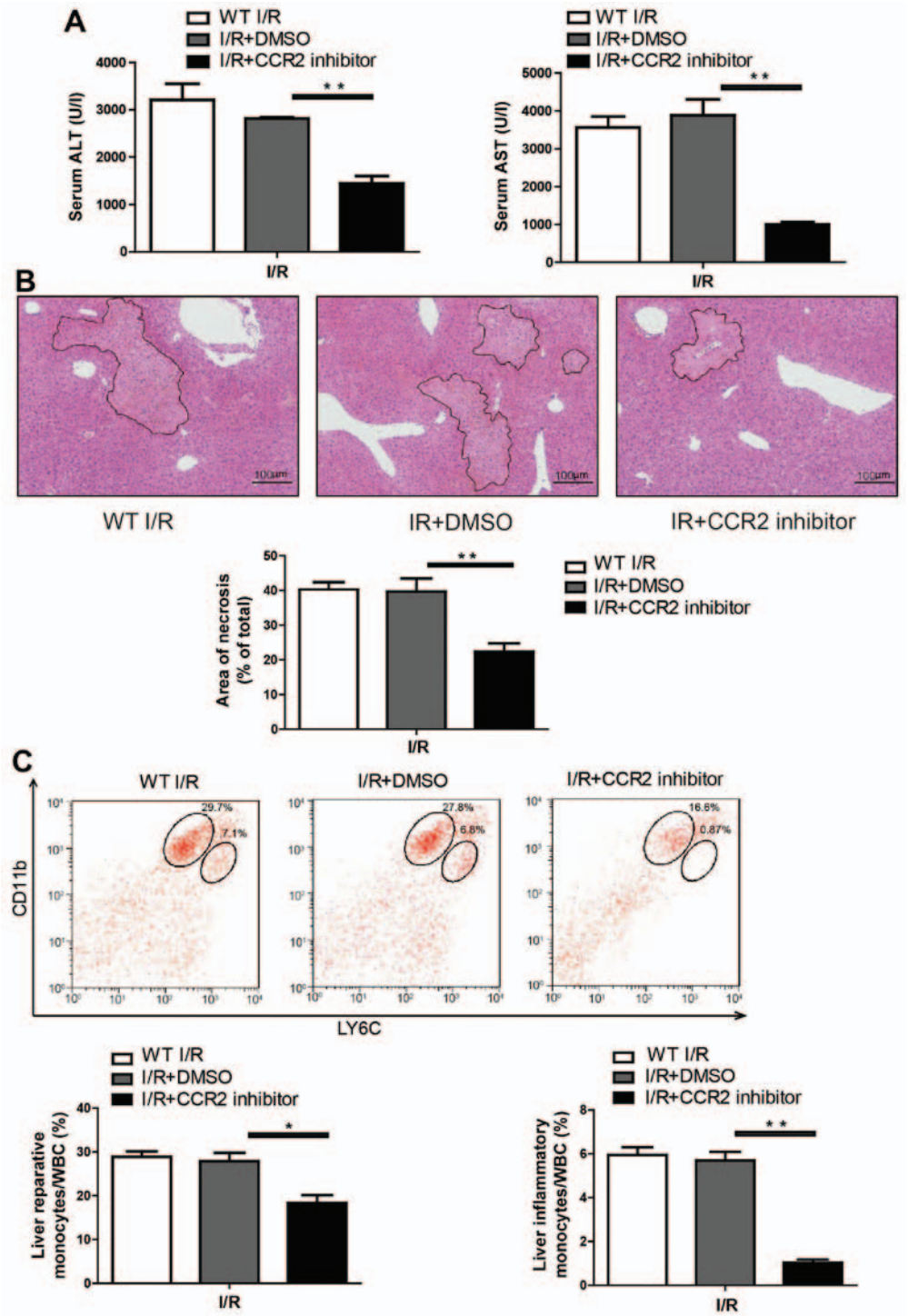

Figure 7. Effect of CCR2 inhibition on hepatic I/R injury. WT mice were pretreated with vehicle (DMSO) or CCR2 inhibitor RS504393 (n=4-6 mice/group) and then subjected to I/R. (A) Serum ALT and AST levels. (B) Areas of necrosis in liver. (C) Flow cytometric analysis of reparative monocytes (CD11b$^+$ Ly6C low) and inflammatory monocytes (CD11b$^+$ Ly6C high) in liver. *P<0.05 and **P<0.01. WT, wild-type; I/R, ischemia/reperfusion; DMSO, dimethyl sulfoxide; CCR2, C-C chemokine receptor 2; ALT, alanine aminotransferase; AST, aspartate aminotransferase; WBC, white blood cells.

demonstrated to initiate liver injury in infected mice and produced pathogenic TNF (46). By contrast, the accumulation of Ly6C$^-$ monocytes/macrophages in the liver coincided with a drop in the pool of Ly6C$^+$ monocytes and provided hepatoprotective function by secreting the anti-inflammatory cytokine IL-10 (46). The findings of the current study provided evidence of an important role for the recruitment of CD11b$^+$Ly6C$^+$ monocytes to the site of hepatic damage following liver I/R in mice. CD11b$^+$Ly6C^{lo} reparative monocytes are predominantly recruited following acute liver I/R injury, with a lesser extent to CD11b$^+$Ly6C^{hi} inflammatory monocytes. CD11b$^+$Ly6C^{hi} monocytes have been demonstrated to inhibit Th1 differentiation, but enhance development of regulatory T cells and exhibit immunosuppressive characteristics (14). The subsequent release of the inflammatory cytokines, TNF-α and IL-6, in the liver resulted in hepatocyte necrosis and elevated serum ALT and AST levels, which suggest that hepatic injury may be in part due to monocyte infiltration after I/R injury. Therefore, hepatic

infiltration of CD11b$^+$Ly6C^{hi} monocytes may be a self-regulatory mechanism to control inflammation in I/R injury.

The effects of macrophages in monocyte intrahepatic recruitment most likely result from their capacity to express numerous growth factors and cytokines (47). Macrophage depletion can be achieved with the systemic injection of liposomes containing clodronate (37,48). In the current study, ~90% macrophage depletion was successfully achieved in the liver 48 h after a single injection of liposomes containing clodronate. Notably, the transient depletion of macrophages alleviated I/R-induced hepatic damage, coinciding with a ecrease in CD11b$^+$Ly6C$^+$ monocytes intrahepatic infiltration. This finding strongly suggests that macrophages contribute to the damage observed in the liver following I/R injury.

Accumulation of Ly6C^{hi} monocytes in the injured liver is critically dependent on the chemokine receptor CCR2 and its ligand, CCL2 (49). Increasing experimental evidence suggests that CCR2 regulates Ly6C^{hi} monocyte entry into inflamed tissue, albeit indirectly, by promoting the egress of Ly6C^{hi} monocytes from the bone marrow into blood circulation (50). CCR2 critically controls intrahepatic Grl^{hi} monocyte accumulation by mediating their egress from bone marrow (49). The findings of the current study demonstrated that CCR2$^{-/-}$ and CCL2$^{-/-}$ mice had almost no excess intrahepatic infiltration of Ly6C$^+$ monocytes, indicating a similar mechanism applies during liver I/R injury. In addition, upon organ injury, CCR2, CCL2, CCR8 and CCL1 have been previously demonstrated to promote the accumulation of the inflammatory Ly6C$^+$Grl$^+$ monocyte subset as precursors of tissue macrophages in the liver (8). Furthermore, novel anti-CCL2 directed agents specifically blocked the infiltration of pro-inflammatory monocytes into injured murine liver. In the present study, specific CCR2 inhibitor RS504393 was used to pretreat mice prior to I/R injury and produced a magnitude of inhibition similar to that in CCR2$^{-/-}$ deficient mice. CCR2 inhibitor nearly completely suppressed the infiltration of CD11b$^+$Ly6C^{hi} cells into the hepatic tissue following I/R injury. These results suggest that CCR2 inhibition efficiently alleviated the hepatic I/R injury and thus, may be an effective potential drug for hepatic I/R injury. There is a limitation of the current study. Although the internal reference gene β-actin expressed at a high level, there are changes in the expression upon I/R treatment. Therefore, using an additional reference gene would strengthen the reliability and reproducibility of our study.

In conclusion, the current study defined intrahepatic monocyte-derived subsets in experimental murine liver I/R injury and identified that Ly6C$^+$ monocytes have an important role in acute I/R hepatic damage. These findings are likely to be relevant for the treatment of liver disease. CCR2 inhibition alleviated the inflamed hepatic environment, suggesting a potential novel approach for interventions targeting pro-inflammatory actions of Ly6C^{hi} monocytes in the liver following I/R injury. However, translation from animal model into human clinical studies requires further investigation.

Acknowledgements

This study was supported by grants from the National Natural Science Foundation of China (nos. 81070355 and 81570570). We also acknowledge Dr Yin Liu (College of Life Science, Wuhan University, Wuhan, China) for providing technical assistance with flow cytometry.

References

1. Peralta C, Jiménez-Castro MB and Gracia-Sancho J: Hepatic ischemia and reperfusion injury: Effects on the liver sinusoidal milieu. J Hepatol 59: 1094-1106, 2013.
2. Kupiec-Weglinski JW and Busuttil RW: Ischemia and reperfusion injury in liver transplantation. Transplant Proc 37: 1653-1656, 2005.
3. Seki E, De Minicis S, Osterreicher CH, Kluwe J, Osawa Y, Brenner DA and Schwabe RF: TLR4 enhances TGF-beta signaling and hepatic fibrosis. Nat Med 13: 1324-1332, 2007.
4. Jaeschke H: Mechanisms of Liver Injury. II. Mechanisms of neutrophil-induced liver cell injury during hepatic ischemia-reperfusion and other acute inflammatory conditions. Am J Physiol Gastrointest Liver Physiol 290: G1083-G1088, 2006.
5. Abu-Amara M, Yang SY, Tapuria N, Fuller B, Davidson B and Seifalian A: Liver ischemia/reperfusion injury: Processes in inflammatory networks - a review. Liver Transpl 16: 1016-1032, 2010.
6. Ju C and Tacke F: Hepatic macrophages in homeostasis and liver diseases: From pathogenesis to novel therapeutic strategies. Cell Mol Immunol 13: 316-327, 2016.
7. Wang F, Yin J, Lu Z, Zhang G, Li J, Xing T, Zhuang S and Wang N: Limb ischemic preconditioning protects against contrast-induced nephropathy via renalase. EBioMedicine 9: 356-365, 2016.
8. Tacke F: Functional role of intrahepatic monocyte subsets for the progression of liver inflammation and liver fibrosis in vivo. Fibrogenesis Tissue Repair 5 (Suppl 1): S27, 2012.
9. Dai LJ, Li HY, Guan LX, Ritchie G and Zhou JX: The therapeutic potential of bone marrow-derived mesenchymal stem cells on hepatic cirrhosis. Stem Cell Res 2: 16-25, 2009.
10. Klein I, Cornejo JC, Polakos NK, John B, Wuensch SA, Topham DJ, Pierce RH and Crispe IN: Kupffer cell heterogeneity: Functional properties of bone marrow derived and sessile hepatic macrophages. Blood 110: 4077-4085, 2007.
11. Tacke F and Randolph GJ: Migratory fate and differentiation of blood monocyte subsets. Immunobiology 211: 609-618, 2006.
12. Tacke F, Alvarez D, Kaplan TJ, Jakubzick C, Spanbroek R, Llodra J, Garin A, Liu J, Mack M, van Rooijen N, *et al*: Monocyte subsets differentially employ CCR2, CCR5, and CX3CR1 to accumulate within atherosclerotic plaques. J Clin Invest 117: 185-194, 2007.
13. Combadière C, Potteaux S, Rodero M, Simon T, Pezard A, Esposito B, Merval R, Proudfoot A, Tedgui A and Mallat Z: Combined inhibition of CCL2, CX3CR1, and CCR5 abrogates Ly6C(hi) and Ly6C(lo) monocytosis and almost abolishes atherosclerosis in hypercholesterolemic mice. Circulation 117: 1649-1657, 2008.
14. Ma H, Wan S and Xia CQ: Immunosuppressive CD11b$^+$Ly6C^{hi} monocytes in pristane-induced lupus mouse model. J Leukoc Biol 99: 1121-1129, 2016.
15. Neal LM and Knoll LJ: Toxoplasma gondii profilin promotes recruitment of Ly6C^{hi} CCR2$^+$ inflammatory monocytes that can confer resistance to bacterial infection. PLoS Pathog 10: e1004203, 2014.
16. Helk E, Bernin H, Ernst T, Ittrich H, Jacobs T, Heeren J, Tacke F, Tannich E and Lotter H: TNFα-mediated liver destruction by Kupffer cells and Ly6C^{hi} monocytes during Entamoeba histolytica infection. PLoS Pathog 9: e1003096, 2013.
17. Marra F, DeFranco R, Grappone C, Milani S, Pastacaldi S, Pinzani M, Romanelli RG, Laffi G and Gentilini P: Increased expression of monocyte chemotactic protein-1 during active hepatic fibrogenesis: Correlation with monocyte infiltration. Am J Pathol 152: 423-430, 1998.
18. Denney L, Kok WL, Cole SL, Sanderson S, McMichael AJ and Ho LP: Activation of invariant NKT cells in early phase of experimental autoimmune encephalomyelitis results in differentiation of Ly6C^{hi} inflammatory monocyte to M2 macrophages and improved outcome. J Immunol 189: 551-557, 2012.
19. Gibbons MA, MacKinnon AC, Ramachandran P, Dhaliwal K, Duffin R, Phythian-Adams AT, van Rooijen N, Haslett C, Howie SE, Simpson AJ, *et al*: Ly6C^{hi} monocytes direct alternatively activated profibrotic macrophage regulation of lung fibrosis. Am J Respir Crit Care Med 184: 569-581, 2011.

20. Shimizu Y, Murata H, Kashii Y, Hirano K, Kunitani H, Higuchi K and Watanabe A: CC-chemokine receptor 6 and its ligand macrophage inflammatory protein 3alpha might be involved in the amplification of local necroinflammatory response in the liver. Hepatology 34: 311-319, 2001.
21. Baeck C, Wehr A, Karlmark KR, Heymann F, Vucur M, Gassler N, Huss S, Klussmann S, Eulberg D, Luedde T, *et al*: Pharmacological inhibition of the chemokine CCL2 (MCP-1) diminishes liver macrophage infiltration and steatohepatitis in chronic hepatic injury. Gut 61: 416-426, 2012.
22. Haukeland JW, Damås JK, Konopski Z, Løberg EM, Haaland T, Goverud I, Torjesen PA, Birkeland K, Bjøro K and Aukrust P: Systemic inflammation in nonalcoholic fatty liver disease is characterized by elevated levels of CCL2. J Hepatol 44: 1167-1174, 2006.
23. Klueh U, Czajkowski C, Ludzinska I, Qiao Y, Frailey J and Kreutzer DL: Impact of CCL2 and CCR2 chemokine/receptor deficiencies on macrophage recruitment and continuous glucose monitoring in vivo. Biosens Bioelectron 86: 262-269, 2016.
24. Yadav A, Saini V and Arora S: MCP-1: chemoattractant with a role beyond immunity: a review. Clin Chim Acta 411: 1570-1579, 2010.
25. Zhao L, Lim SY, Gordon-Weeks AN, Tapmeier TT, Im JH, Cao Y, Beech J, Allen D, Smart S and Muschel RJ: Recruitment of a myeloid cell subset (CD11b/Gr1 mid) via CCL2/CCR2 promotes the development of colorectal cancer liver metastasis. Hepatology 57: 829-839, 2013.
26. Braunersreuther V, Viviani GL, Mach F and Montecucco F: Role of cytokines and chemokines in non-alcoholic fatty liver disease. World J Gastroenterol 18: 727-735, 2012.
27. Castellaneta A, Yoshida O, Kimura S, Yokota S, Geller DA, Murase N and Thomson AW: Plasmacytoid dendritic cell-derived IFN-α promotes murine liver ischemia/reperfusion injury by induction of hepatocyte IRF-1. Hepatology 60: 267-277, 2014.
28. Le Page S, Niro M, Fauconnier J, Cellier L, Tamareille S, Gharib A, Chevrollier A, Loufrani L, Grenier C, Kamel R, *et al*: Increase in Cardiac Ischemia-Reperfusion Injuries in Opa1$^{+/-}$ Mouse Model. PLoS One 11: e0164066, 2016.
29. Wei Q and Dong Z: Mouse model of ischemic acute kidney injury: Technical notes and tricks. Am J Physiol Renal Physiol 303: F1487-F1494, 2012.
30. Wilson GC, Freeman CM, Kuethe JW, Quillin RC III, Nojima H, Schuster R, Blanchard J, Edwards MJ, Caldwell CC and Lentsch AB: CXC chemokine receptor-4 signaling limits hepatocyte proliferation after hepatic ischemia-reperfusion in mice. Am J Physiol Gastrointest Liver Physiol 308: G702-G709, 2015.
31. Andrassy M, Volz HC, Igwe JC, Funke B, Eichberger SN, Kaya Z, Buss S, Autschbach F, Pleger ST, Lukic IK, *et al*: High-mobility group box-1 in ischemia-reperfusion injury of the heart. Circulation 117: 3216-3226, 2008.
32. Inoue Y, Shirasuna K, Kimura H, Usui F, Kawashima A, Karasawa T, Tago K, Dezaki K, Nishimura S, Sagara J, *et al*: NLRP3 regulates neutrophil functions and contributes to hepatic ischemia-reperfusion injury independently of inflammasomes. J Immunol 192: 4342-4351, 2014.
33. Livak KJ and Schmittgen TD: Analysis of relative gene expression data using real-time quantitative PCR and the 2(-Delta Delta C(T)) Method. Methods 25: 402-408, 2001.
34. He L, Sun F, Wang Y, Zhu J, Fang J, Zhang S, Yu Q, Gong Q, Ren B, Xiang X, *et al*: HMGB1 exacerbates bronchiolitis obliterans syndrome via RAGE/NF-κB/HPSE signaling to enhance latent TGF-β release from ECM. Am J Transl Res 8: 1971-1984, 2016.
35. Duret C, Gerbal-Chaloin S, Ramos J, Fabre JM, Jacquet E, Navarro F, Blanc P, Sa-Cunha A, Maurel P and Daujat-Chavanieu M: Isolation, characterization, and differentiation to hepatocyte-like cells of nonparenchymal epithelial cells from adult human liver. Stem Cells 25: 1779-1790, 2007.
36. Van Rooijen N and Hendrikx E: Liposomes for specific depletion of macrophages from organs and tissues. Methods Mol Biol 605: 189-203, 2010.
37. Van Rooijen N and Sanders A: Liposome mediated depletion of macrophages: Mechanism of action, preparation of liposomes and applications. J Immunol Methods 174: 83-93, 1994.
38. Lv Q, Yang F, Chen K and Zhang Y: Autophagy protects podocytes from sublytic complement induced injury. Exp Cell Res 341: 132-138, 2016.
39. Rossi L, Serafini S, Antonelli A, Pierigé F, Carnevali A, Battistelli V, Malatesta M, Balestra E, Caliò R, Perno CF, *et al*: Macrophage depletion induced by clodronate-loaded erythrocytes. J Drug Target 13: 99-111, 2005.
40. Heymann F, Trautwein C and Tacke F: Monocytes and macrophages as cellular targets in liver fibrosis. Inflamm Allergy Drug Targets 8: 307-318, 2009.
41. Sullivan T, Miao Z, Dairaghi DJ, Krasinski A, Wang Y, Zhao BN, Baumgart T, Ertl LS, Pennell A, Seitz L, *et al*: CCR2 antagonist CCX140-B provides renal and glycemic benefits in diabetic transgenic human CCR2 knockin mice. Am J Physiol Renal Physiol 305: F1288-F1297, 2013.
42. Wang F, Zhang G, Lu Z, Geurts AM, Usa K, Jacob HJ, Cowley AW, Wang N and Liang M: Antithrombin III/SerpinC1 insufficiency exacerbates renal ischemia/reperfusion injury. Kidney Int 88: 796-803, 2015.
43. Brempelis KJ and Crispe IN: Infiltrating monocytes in liver injury and repair. Clin Transl Immunology 5: e113, 2016.
44. Höchst B, Mikulec J, Baccega T, Metzger C, Welz M, Peusquens J, Tacke F, Knolle P, Kurts C, Diehl L, *et al*: Differential induction of Ly6G and Ly6C positive myeloid derived suppressor cells in chronic kidney and liver inflammation and fibrosis. PLoS One 10: e0119662, 2015.
45. Cuervo H, Guerrero NA, Carbajosa S, Beschin A, De Baetselier P, Gironès N and Fresno M: Myeloid-derived suppressor cells infiltrate the heart in acute Trypanosoma cruzi infection. J Immunol 187: 2656-2665, 2011.
46. Morias Y, Abels C, Laoui D, Van Overmeire E, Guilliams M, Schouppe E, Tacke F, deVries CJ, De Baetselier P and Beschin A: Ly6C$^-$ monocytes regulate parasite-induced liver inflammation by inducing the differentiation of pathogenic Ly6C$^+$ monocytes into macrophages. PLoS Pathog 11: e1004873, 2015.
47. Alisi A, Carpino G, Oliveira FL, Panera N, Nobili V and Gaudio E: The role of tissue macrophage-mediated inflammation on NAFLD pathogenesis and its clinical implications. Mediators Inflamm 2017: 8162421, 2017.
48. Weisser SB, van Rooijen N and Sly LM: Depletion and reconstitution of macrophages in mice. J Vis Exp: Aug 1, 2012. (Epub ahead of print). doi: 10.3791/4105.
49. Karlmark KR, Weiskirchen R, Zimmermann HW, Gassler N, Ginhoux F, Weber C, Merad M, Luedde T, Trautwein C and Tacke F: Hepatic recruitment of the inflammatory Gr1$^+$ monocyte subset upon liver injury promotes hepatic fibrosis. Hepatology 50: 261-274, 2009.
50. Engel DR, Maurer J, Tittel AP, Weisheit C, Cavlar T, Schumak B, Limmer A, van Rooijen N, Trautwein C, Tacke F, *et al*: CCR2 mediates homeostatic and inflammatory release of Gr1(high) monocytes from the bone marrow, but is dispensable for bladder infiltration in bacterial urinary tract infection. J Immunol 181: 5579-5586, 2008.